Phenomenological theory of lattice dynamics and polymorphism of ZrO_2

M. Smirnov,[1] A. Mirgorodsky,[2,*] and R. Guinebretière[3]
[1]*Fock Institute of Physics, Saint-Petersburg University, 194508 Petrodvoretz, St.-Petersburg, Russia*
[2]*Science des Procédés Céramiques et de Traitements de Surface UMR 6638, Faculté des Sciences et Techniques, 123 avenue Albert Thomas, 87060 Limoges Cedex, France*
[3]*Science des Procédés Céramiques et de Traitements de Surface UMR 6638, ENSCI, 47-73 avenue Albert Thomas, 87065 Limoges Cedex, France*

(Received 8 August 2002; revised manuscript received 11 February 2003; published 8 September 2003)

The cubic-tetragonal-monoclinic structural evolution of zirconia (ZrO_2) is studied within a lattice dynamical treatment using a model approach taking into consideration the variability of the oxygen ion charge. The relevant calculations reveal the two physical factors driving that evolution. A specific Zr/O ionic radii ratio is one of them: the radius of Zr^{4+} is found to be too small to ensure stability of the ZrO_8 cube, but not sufficiently small to ensure the stability of the ZrO_6 octahedron. Thus, the ZrO_7 coordination polyhedron arises as a basic structural fragment specifying the monoclinic (baddeleyite) lattice. Another factor is the dependence of an ionic charge on its local environment in the crystal. This results in the charge redistribution between nonequivalent oxygen ions during the structural transformations, which is found to be indispensable to stabilize the baddeleyite lattice as a ground-state structure of zirconia. Special attention is paid to the elastic anomalies accompanying the tetragonal-monoclinic transition, which were never considered in the preceding studies. According to the present work, those anomalies are related to the intermediate orthorhombic structure (D_{2h}^{8}, No. 54) which is characterized as essentially unstable.

DOI: 10.1103/PhysRevB.68.104106 PACS number(s): 61.50.Ah, 63.20.Dj, 64.60.−i

I. INTRODUCTION

The structural phase transfomations (SPT's) in crystalline zirconia manifest a number of properties,[1,2] which are of great engineering importance and of high interest for solid state physics. The most intriguing one is the transition from the monoclinic (*m*) phase to the tetragonal (*t*) phase ($T = 1450$ K) which is accompanied by a spontaneous volume reduction of approximately 4.5%. Subsequently, tetragonal zirconia can undergo a SPT into a cubic (*c*) phase with fluoritelike structure, induced by heating ($T = 2650$ K), i.e., with volume extension, or by hydrostatic pressure,[3] i.e., with volume contraction. Another particularity of zirconia is the structure of its ground-state *m* phase (baddeleyite) in which zirconium atoms have an odd (sevenfold) coordination, and the two nonequivalent (three-coordinated and four-coordinated) oxygen atom positions occur. Many experimental studies were devoted to the polymorphism of zirconia, and most of their results remain a challenge for the theory. This can be explained partly by the absence of an adequate potential function model. Numerous attempts to develop such a model[4–11] failed to describe the stability of the baddeleyite structure. This explains why recent attention has been paid to theoretical studies based on quantum-mechanical (QM) *ab initio* calculations.[12–21] Such calculations are rather laborious, and have been primarily restricted to static energy surface analysis.

The *ab initio* theory shows that the absolute minimum of the zirconia's potential surface corresponds to the baddeleyite lattice.[17] The energy minimization in the cubic, tetragonal, and monoclinic phases led to structures with molar volumes $V_c < V_t < V_m$ and with the specific energy $E_c > E_t > E_m$, respectively. The volume dependence of the calculated static energy for all these phases is shown in Fig. 1. Little else in terms of information was obtained from the quantum-mechanical potential energy studies. The stability of the phases as a function of the volume variation was not comprehensively explored. The phonon dispersion of the *c* phase was calculated at $V = V_c$ only.[19,20] The study of the phonon states in the *t* phase was limited by the Γ point calculation at $V = V_t$.[21] Nothing is known about the phonon states at the *M* point which must play a key role in the *t*-*m* instability.[22] The evolution of the simulated phonon spectrum with volume variation was never reported.

The point at which the $E(V)$ curves of two phases approach each another (see, e.g., Fig. 1), is of particular interest for phase transition theory. Actually, on each side of such a point, the phase with a higher energy would be unstable. In

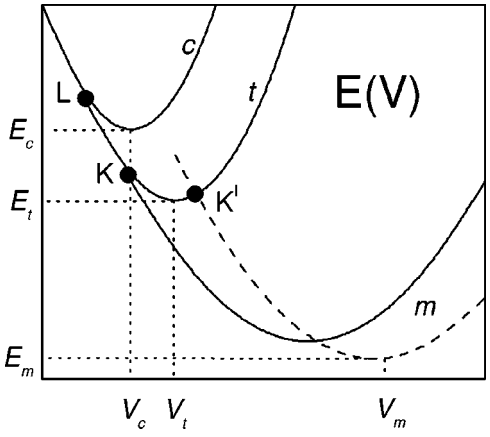

FIG. 1. Energy versus volume dependence of the three main zirconia polymorphs, schematically designed according to results of the *ab initio* studies of Ref. 16 (solid lines) and those of Ref. 17 (dashed lines).

principle, the phonon state and the elastic constant calculations could reveal the atomic displacement pattern related to these instabilities, thus giving a microscopic insight into the phase transition mechanism. However, this problem was never examined in the quantum-mechanical studies of zirconia. Frequently, the $E(V)$ curves were plotted by using an analytic approximation formula, and the physical sense of their intersections was thus lost. Therefore, a static energy analysis in the quantum-mechanical studies of zirconia did not provide much important information about the phenomena under consideration. This is partly due to computational difficulties inherent for *ab initio* studies, which become even greater in a finite-temperature free-energy analysis. Therefore, the necessity of an appropriate potential model of ZrO_2 remains paramount.

In the last decade, a number of oxide structures, including the rather covalent compound SiO_2,[23] were successfully simulated using the ionic model. Consequently there is no reason to suppose that this model is not applicable in the case of ZrO_2. The high and variable value of the coordination number of the Zr atom in ZrO_2 indicates an essentially ionic character of binding in this crystal. However, the attempts to apply this model to ZrO_2 have regularly failed. The absolute energy minimum appeared either in the cubic fluoritelike structure or in an ''octahedral'' structure with sixfold coordination of Zr atoms, which has never been observed in ZrO_2. The inclusion of the ionic polarizability in the model did not improve the situation.

It is useful to recall that the the baddeleyite structures of dioxides are stable only with the medium-sized cations Zr and Hf, whereas the dioxide fluoritelike lattices (with eightfold cation coordination) are stable with larger cations (Th, Ce, U), and the dioxide structures with sixfold cation coordination are stable with smaller cations (Pb, Sn, Ti, W).

We then deduce that the failure of the previous attempts to apply the ionic potential model to zirconia was caused not by inadequacy of the ionic concept but by specific relations between the atomic characteristics in this compound. In particular, the ratio of the ionic radii of cations and anions is peculiar to ZrO_2 , which results in a mutual compensation of the two main potential energy contributions and therefore, the structures with different coordination numbers have comparable energy values (see Sec. II) Consequently, other contributions in the potential function, which are not so significant in most oxides, dominate the lattice dynamics and induce the structural transformations. The results of the present paper show that this is the case for ZrO_2. Previous works have suggested (Refs. 5,10) that the variability of the oxygen ion radius could specify the mechanism of such transformations. However, its inclusion in the model did not ensure the stability of the baddeleyite structure.[24]

In our opinion, to reveal the main factors governing the *c-t-m* evolution of the zirconia lattice, one should not propose various *ad hoc* potential function contributions but rather try to understand the objective factors inducing the structural instability in the cubic and tetragonal phases of ZrO_2. This can be done through an analysis of the microscopic nature of these instabilities by focusing attention on the softness of the specific degrees of freedom (the phonon modes and the elastic strains), whose relaxation would cause the stabilization of the baddeleyite structure. This is the main goal of the present paper.

II. MODEL

On developing our model, we attempted first of all to reproduce the experimental data and to fulfil the following three conditions discovered in the *ab initio* studies of the potential surface of zirconia:

Condition 1: The absolute energy minimum corresponds to the *m* phase with baddeleyite structure.

Condition 2: The energy versus volume dependence for the three zirconia polymorphs is close to that shown in Fig. 1.

Condition 3: The energy of the highest-symmetry *c* phase is lower than that of all the hypothetical crystal structures with the sixfold cation coordination (such as rutile, anatase, brookite, α-PbO_2).

Starting from the simplest ionic model [rigid ion model (RIM)], we first explored the questions: which of the just mentioned Conditions can it obey, and why it cannot fulfil the others? Then, after discovering the source of the model's shortcoming, its necessary improvements were made. Finally, any term in thus developed potential model was unequivocally determined by a physical characteristic detected in the QM calculations or in the experimental studies.

Within RIM, the two main contributions to the potential energy correspond to the Coulomb interaction and to the short-range overlap repulsion. They are presented in the Born-Meyer potential as follows:

$$E = \frac{1}{2}\sum_{i\neq j}\left[\frac{Z_i Z_j}{r_{ij}} + A\exp\left(-\frac{r_{ij}}{\rho}\right)\right]. \tag{1}$$

On assuming the formal ionic charge values Zr^{4+} and O^{2-} and on supposing the overlap repulsion to be significant between cations and anions only, one has to determine only the two repulsion parameters A and ρ. These parameters are directly related through the ionic radii of cation R^+ and anion R^-. In Ref. 25 this relation was expressed as follows :

$$A = \varepsilon\,\exp\left(\frac{R^+ + R^-}{\rho}\right) \tag{2}$$

with ε defined somewhat arbitrarily as a typical rate of the atomic binding energy. We put the ε value equal to 2.3 aJ, i.e., to the Coulomb energy of the charges $+1e$ and $-1e$ separated by the distance of 1 Å. The sum $L = R^+ + R^-$ is referred below as the effective radius of the Zr-O interaction. This quantity (rather than A) offers a simple physical interpretation of the overlap repulsion. Its magnitude must reflect the fact that ZrO_2 is an intermediate case between the dioxides with cations larger than Zr, which are stable in the eightfold coordinated cubic structure, and the dioxides with cations smaller than Zr, which are stable in the sixfold cation coordination.

In line with the *ab initio* results,[16,17] we assumed that the energy of the *c* phase is minimal at a Zr-O bond length of 2.2

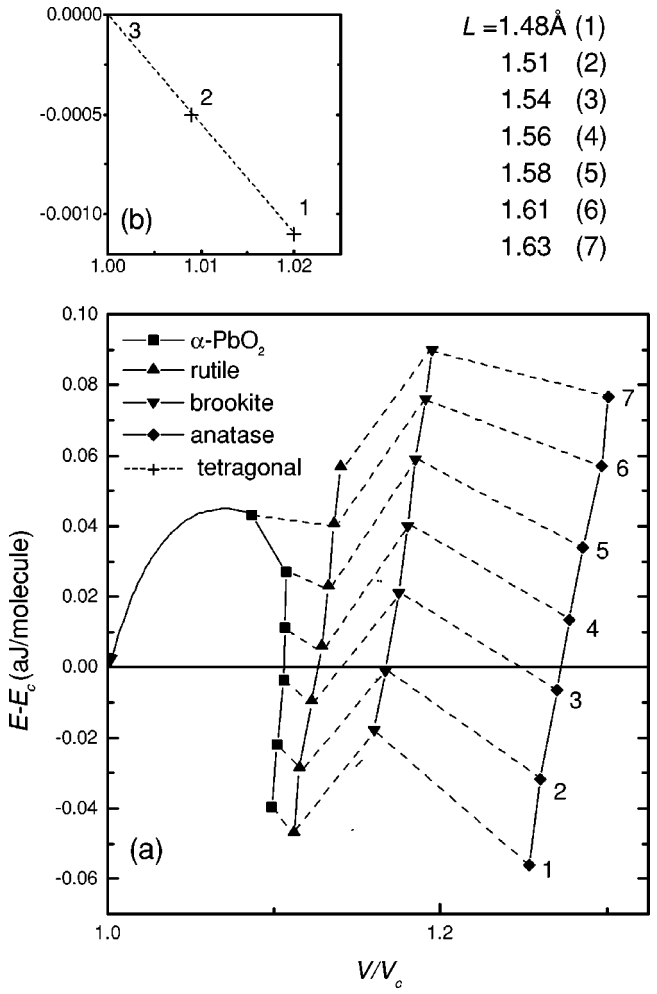

FIG. 2. RIM: relative positions of the energy minima of different crystal structures in dependence of the effective radius L (in Å). (a) Fluorite and the ''octahedral'' structures; (b) tetragonal phase.

Å. This imposed a constraint which established a one-to-one relation between the possible L and ρ values. This relation was used to determine the ρ values for the different magnitudes of L value varied in the interval 1.48–1.63 Å. With the potential parameters thus found, the energy minimum configurations for the relevant crystal structures under consideration were determined, and their energy was compared with that of the c phase. These results, shown in Fig. 2 , allowed us to determine the critical L value which ensures the above mentioned Condition 3. The following is seen from Fig. 2.

At $L>1.55$ Å (versions 4–7) the absolute energy minimum corresponds to the c-phase structure (i.e., the points corresponding to all other structures are above the abscissa axis in Fig. 2).

At $L<1.55$ Å (versions 1–3) the energy of the structures with the sixfold cation coordination is lower than that of the c phase (at L over the interval 1.52–1.55 Å the ground state structure is rutile, and at L in the range 1.40–1.52 Å the ground state structure is anatase).

Note, that at $L<1.40$ Å, the ground-state structure corresponds to the quartzlike lattice with the fourfold coordination of cations. This interval of the model parameters does not bear on our analysis.

So, it is sufficient to suppose that the L value in the potential function of ZrO_2 must be slightly higher than 1.55 Å in order to fulfill condition 3. We put $L=1.605$ Å. This leads to $E_{\text{rutile}}-E_c=0.043$ aJ/molecule, which agrees well with the *ab initio* estimation $E_{\text{rutile}}-E_c=0.048$ aJ/molecule, drawn from the curves shown in Ref. 16. The corresponding parameters of the potential presented by Eq. (1) are $A=258$ aJ and $\rho=0.34$ Å.

Condition 2 implies that the fluorite structure of ZrO_2 must be unstable with respect to c-t distortion. However, the calculation within RIM showed [see Fig. 2(b)] that this instability occurs at the same L values which provide the ground state structure with the sixfold cation coordination. So, RIM is incapable of obeying all the above implied conditions, and it is inevitable to add a mechanism amplifying the c-t instability.

The quantitative criterion of this instability is the imaginary frequency of the X_2^- mode in the c phase.[26] The eigenvector of this mode involves the antiphase displacements of the neighboring columns $\ldots -\mathrm{O}-\mathrm{O}-\ldots$, and the stiffness of this distortion depends strongly on the ionic polarizability.[10] So, the model improvement can be done by using the polarizable ion approximation within the shell model (SM).[27] Customarily, only the anion polarizability is taken into account, and the extension of RIM to SM involves the two additional parameters: oxygen ion polarizability α and shell charge Y. Their values were chosen as $\alpha(\mathrm{O}^{2-})=1.2$ Å^3 and $Y(\mathrm{O}^{2-})=-4e$, which ensured the occurrence of c-t instability and led to the calculated frequencies $\omega(X_2^-)=i129$ cm^{-1} and $\omega(F_{1u})=330$ cm^{-1}, whereas the *ab initio* results[19,20] gave $i195$ cm^{-1} and 269 cm^{-1}, respectively. [Note, that the experimental value of TO-mode frequency $\omega(F_{1u})$ is 320 cm^{-1} (Ref. 28).] The effective dynamic charge calculated within this SM is of $4.5e$. Its *ab initio* value was found of $5.75e$.[20] So, the ionic model including the oxygen ion polarizability is capable of reproducing the occurrence of c-t instability, and at the same time, of obeying the third of the above conditions. The latter point is fulfilled because the oxygen ion polarization does not affect the energy of the c phase and very slightly affects the energy of the ''octahedral'' crystal structures.

This is not the case for the t phase. The ionic polarization plays a key role in c-t instability and determines the magnitude of c-t distortion (described by the oxygen position displacement parameter Δz) at $V=V_c$. The chosen value of $\alpha(\mathrm{O}^{2-})$ reproduces the $\omega(X_2^-)$ frequency well (i.e., the curvature of the double-well potential governing the c-t distortion) but overestimates the c-t energy barrier and the magnitude of the geometry distortion. This necessitates a further improvement of the model involving the ionic polarization nonlinearity. In doing this, we supposed the core-shell potential to differ from a harmonic one. Traditionally, the core-shell potential is represented by the harmonic law $U(s)=ks^2/2$,[27] in which s is the core-shell displacement, and $k=Y^2/\alpha$ is the core-shell spring stiffness. The potential used in our study is

$$U(s)=kd^2\left[\cosh\left(\frac{s}{d}\right)-1\right]=\frac{ks^2}{2}\left[1+\frac{1}{12}\left(\frac{s}{d}\right)^2+\cdots\right], \quad (3)$$

TABLE I. Energy minimum characteristics of the three zirconia polymorphs.

Volume (Å^3/molecule)			c-t distortion	Energy barrier (10^{-21} J/molecule)		Method and
V_c	V_t	V_m	Δz	ΔE_{tc}	ΔE_{mt}	reference
33.1	33.5	35.0	0.033	5	12	*ab initio* (Ref. 16)
34.3	35.9	37.1	0.050	13	16	*ab initio* (Ref. 17)
32.9	33.7	35.1	0.06	9	10	Exp. (Ref. 2)
32.7	33.1	35.2	0.039	2.6	2.5	VCM, this work

which means that the ionic polarizability decreases with increasing ionic polarization. The new parameter d determines a critical core-shell displacement, above which this nonlinearity comes into prominence. Its value was chosen to reproduce the t-phase energy minimum configuration found in the *ab initio* studies (see Table I).

Finally, we have concentrated on the questions: what is the basic reason for stability of the baddeleyite structure and why is the traditional ionic model incapable of reproducing it? The answer to these questions seems to be suggested by the fact that the baddeleyite structure has the two essentially different oxygen ion positions. A half of them (O^I) are situated in the center of the threefold star O^IZr_3, just as in the ''octahedral'' crystal structures. The other oxygen position (O^{II}) is located in the center of the slightly distorted tetrahedron $O^{II}Zr_4$, similar to that in the fluoritelike structure. It is reasonable to assume that the electron density distribution in these two sites differ markedly. This should be reflected in different values of the ionic parameters for the O^I and O^{II} ions. The idea of different ionic radii of the O^I and O^{II} ions was used in the earlier model treatments of zirconia,[5,10] but it did not favor the explanation of the baddeleyite structure stability. The assumption of different effective charges of the O^I and O^{II} ions was never employed. However, the *ab initio* electron density analysis reveals the considerable difference in the Mulliken charge values for the O^I and O^{II} ions: $Z(O^I)-Z(O^{II})\simeq 0.2e$.[28] Being multiplying by the difference in the Madelung potentials $\varphi(O^{II})-\varphi(O^I)=0.089\ e/\text{Å}$ (calculated within the experimental lattice geometry and with the formal ionic charges), this quantity leads to the energy $\Delta E = \Delta Z \Delta\varphi = 0.02$ aJ/molecule. This energy value, gained in course of charge transfer between the O^I and O^{II} ions, is of the same magnitude as the energy barrier $E_t - E_m = 0.016$ aJ/molecule estimated from the results of the *ab initio* calculations.[16]

It is likely that the difference between the charges of the O^I and O^{II} ions is an essential factor for the stability of the baddeleyite structure. Actually, according to our preliminary calculations, this structure can be stable in the framework of an *ad hoc* RIM with different charges on the O^I and O^{II} ions. However, the aim of this study is more complicated. It consists in developing a *self-consistent* model in which the magnitude of the effective ionic charge would adiabatically depend on the local crystal environment. The key idea of our model, which will be called the variable charge model (VCM), is borrowed from the charge equilibrium model, proposed in Ref. 30. Within this model, the magnitude of the effective charge variation.

$$Z_i = Z_i^0 + \Delta Z_i \tag{4}$$

is taken to be proportional to the local electrostatic potential

$$\Delta Z_i \sim c_i \varphi_i . \tag{5}$$

Simply stated, the deeper is the potential well, the more of electron density is located in it. We developed this idea by putting that ionic radius is also a variable quantity

$$R_i = R_i^0 + \Delta R_i , \tag{6}$$

and its variation is proportional to the charge variation

$$\Delta R_i = t_i \Delta Z_i . \tag{7}$$

In the above expressions, Z_i^0 and R_i^0 are the charge and radius values of a ''free'' ion. Similarly to Ref. 30, the effective charge values for any atomic configuration are determined through the minimization of the Hamiltonian:

$$E(r,Z,R) = \sum_i F_i(\Delta Z_i) + \sum_{i\neq j}\left[\frac{Z_i Z_j}{r_{ij}} + \varepsilon \exp\left(\frac{R_i + R_j - r_{ij}}{\rho}\right)\right], \tag{8}$$

where term $F_i(\Delta Z_i)$ describes the energy variation due to the charge redistribution. On neglecting the ionic radius variation, the minimization of E with respect to ΔZ_i leads to the equation

$$\frac{dF_i}{d\Delta Z_i} = -\Delta Z_i \varphi_i . \tag{9}$$

To make it identical to Eq. (5), one has to define the $F_i(\Delta Z_i)$ function as

$$F_i = \frac{1}{2c_i}\Delta Z_i^2 . \tag{10}$$

Thus, the relations (4)–(8), (10) together with the charge neutrality condition

$$\sum_i Z_i = 0 \tag{11}$$

could determine the analytic scope of the model. However, a numerical test showed that a low scale nonlinearity in the dependence (5) is necessary in order to limit the charge redistribution process. Analogously to Eq. (3), Eq. (10) is substituted by the relation:

TABLE II. Geometry parameters of the *m* phase of ZrO2.

	exp. (Ref. 2)	*ab initio* (Ref. 17)	VCM, this work
a,b,c(Å)	5.145, 5.210, 5.312	5.242, 5.305, 5.410	5.167, 5.157, 5.323
$\beta(^\circ)$	99.2	99.23	97.2
Zr	0.2751, 0.0404, 0.2081	0.2765, 0.0421, 0.2090	0.2806, 0.0176, 0.2194
O^{I}	0.0770, 0.3351, 0.3437	0.071, 0.337, 0.342	0.0468, 0.2973, 0.3812
O^{II}	0.5480, 0.2454, 0.5250	0.550, 0.242, 0.521	0.5303, 0.2470, 0.5163
Zr-O^{I} (Å)	2.0371, 2.0838, 2.1391	2.0915, 2.1017, 2.1972	2.0533, 2.0974, 2.2620
Zr-O^{II} (Å)	2.1446, 2.1548, 2.2548, 2.2782	2.1923, 2.2067, 2.2919, 2.2963	2.0969, 2.1412, 2.2117, 2.2818

$$F_i(\Delta Z_i)=\frac{\delta_i^2}{c_i}\left[\cosh\left(\frac{\Delta Z_i}{\delta_i}\right)-1\right]$$
$$=\frac{1}{2c_i}\Delta Z_i^2\left[1+\frac{1}{12}\left(\frac{\Delta Z_i}{\delta_i}\right)^2+\cdots\right], \qquad (12)$$

in which the δ_i parameter determines the limit of the possible charge variation.

Finally, the improvement of the ionic model is determined by relations (4)–(8), (11),(12), whereas the ionic polarization terms stay the same as in a standard SM version.[27] It was supposed that the charge redistribution, as well as the overlap repulsion, operates between the shells but not between the cores, and the c_i coefficients differ from infinity merely for anions. So, the charge transfer between cations and anions is not taken into account, and only the charge transfer between nonequivalent oxygen ions is considered. The charge transfer between oxygen atoms does not change the static energy of the cubic and tetragonal phases, as well as that of all the ''octahedral'' structures, in which all the oxygen positions are equivalent. But it affects the values of the first and second derivatives of the energy with respect to the nonsymmetric atomic displacements leading to the oxygen position nonequivalency. Within VCM, the bare ionic charges Z_i^0 and the overlap repulsion parameters ρ and A were taken the same as in the above discussed SM. The new parameters c_i and t_i, governing the ionic charge and radius variations, were estimated by the auxiliary *ab initio* study of the electronic density distribution in the finite clusters $[OZr_4]^{14+}$ and $[OZr_3]^{10+}$. Finally, their values were slightly fitted in order to make the simulated baddeleyite structure more close to the experimental one. The total set of the model parameters is as follows:

RIM [Eq. (1)]: $Z^0(O)=-2e$, $A=258$ aJ, $\rho=0.34$ Å,

SM [Eq. (3): $Y(O)=-4e$, $k=30$ aJ/Å^2, $d=0.02$ Å,

VCM (Eqs. (4)–(8), (11),(12)]: $c=2.77$ Å,

$t=0.196$ Å$/e$, $\delta=0.35e$.

III. RESULTS AND DISCUSSION

The proposed model reproduces the main characteristics of the potential surface discovered in the *ab initio* studies.

(a) The model provides an absolute energy minimum in the *m*-phase structure close to that observed experimentally and to that obtained in the *ab initio* study (see Table II). Despite of incorrect ratio of the cell parameters *a* and *b*, the main peculiarity of the baddeleyite structure—the threefold coordination of the O^{I} atom and the fourfold coordination of the O^{II} atom—is well described. The charge transfer between oxygen atoms in O^{I} and O^{II} positions plays the key role in stabilizing this structure. The effective ionic charges predicted by our model are $Z(O^{I})=-1.8e$ and $Z(O^{II})=-2.2e$. The magnitude and the sign of the charge redistribution agrees with the *ab initio* estimation of the Mulliken charge difference $Z(O^{I})-Z(O^{II})\simeq 0.2e$.[29]

(b) The $E(V)$ curves calculated within our model for *c*, *t*, and *m* phases (see Fig. 3) agree with those found in the *ab initio* calculations. The positions of the energy minima are presented in Table I. It is seen that the calculated V_c, V_t, and V_m values are close to those found in the *ab initio* studies. The energy barriers predicted by the model are underestimated but are of the same order.

(c) The phonon frequencies calculated in the energy minimum configuration of the *c* and *t* phases (see Table III) agree well with both the *ab initio* results and the experimental data.

Reproducing the main results of the *ab initio* studies, the model seems to be quite reliable to answer important questions which remained beyond the earlier works. Let us consider the *c*-*t*-*m* trasformations of zirconia on paying special attention to the structural instabilities related to the points in which the $E(V)$ curves in Fig. 3 approach each other.

At decreasing volume the $E_c(V)$ and $E_t(V)$ curves approach each other at the L point in which $E_c(V)=E_t(V)$. This indicates a possible pressure-induced *t*-*c* phase transition. Such a continuous phase transformation was observed in Ref. 3 at a hydrostatic pressure interval of 8–30 GPa. Theoretically, the order of this phase transition is related to the character of approaching of $E_c(V)$ and $E_t(V)$ curves. A smooth junction (i.e., with the same derivative at the L point) of those curves would indicate the second-order SPT. Otherwise, this is a first-order SPT for which a triple-minimum potential curve along the *c*-*t* distortion would be inherent.

The potential energy variation governing the *c*-*t* distortion was examined in a series of *ab initio* studies[10,13,14] in which the double-well potential curves have been inevitably found. Moreover, it was shown in those studies that the height of the *c*-*t* energy barrier monotonously decreases at

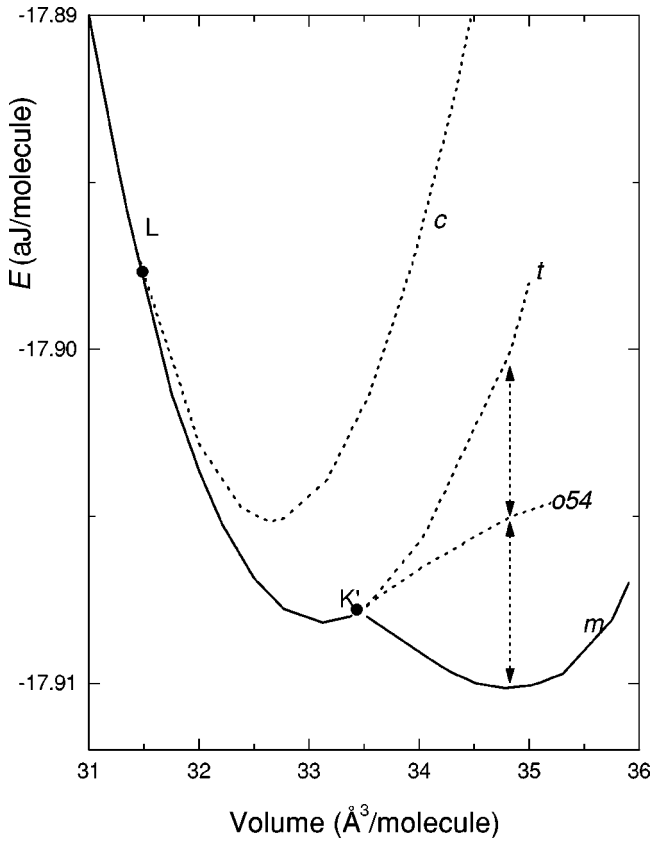

FIG. 3. Potential energy of different crystal phases of ZrO_2 in dependence of the volume variation calculated by VCM. The solid lines correspond to the stable configurations. The unstable configurations, related to saddle points of the potential surface, correspond to the dotted part of the lines.

lattice contraction and eventually vanishes. This unequivocally corresponds to a second-order phase transition and dictates the $E_c(V)$ and $E_t(V)$ curves to be smoothly merging together. Therefore, it may be thought that the crossing of these curves shown in Refs. 17,18 is caused by using some analytic $E(V)$ approximation (as it was explicitly said in Ref. 18) and not by an accurate numerical calculations. Our model (in line with as the *ab initio* study[16]) predicts the $E_c(V)$ and $E_t(V)$ curves as smoothly merging together at $V=31.5$ Å^3/molecule. In this point their slope corresponds to pressure $P_c=12.5$ GPa. The analogous estimation of the critical pressure derived from the $E(V)$ curves presented in Ref. 16 leads to the P_c value of about 35 GPa.

Another experimental fact indicating a possibility of the pressure-induced t-c instability is the negative value of the dT_c/dP derivative estimated as -70 K/GPa in Ref. 34. This quantity can be compared with the calculated ratio $\Delta E_{ct}/\Delta P$, where ΔE_{ct} is expressed in the temperature scale. According to our model, this ratio is equal to -40 K/GPa.

The L point, in which the $E_c(V)$ and $E_t(V)$ curves merge together, corresponds to the volume at which the soft mode X_2^- vanishes. So, the c phase is unstable to the right of the L point in Fig. 3, and this part of the $E_c(V)$ curve (shown by a dotted line) corresponds to the energy surface saddle points with negative curvature along the c-t distortion. In course of this distortion, the c-phase transforms into the t phase. In this phase, the X_2^- mode becomes a totally symmetric A_{1g} mode. Its frequency increases and reaches 219 cm^{-1} in the t-phase energy minimum configuration, according to our model. The volume and pressure dependence of the calculated phonon frequencies in the c and t phases is shown in Fig. 4, in which the value $P=0$ corresponds to the energy minimum configuration of the t phase, and the value $P=12.5$ GPa corresponds to the L point. For the B_{1g}, E_g, and A_{1g} modes presented in Fig. 4, the $d\omega/dP$ coefficients were estimated as 5.1, 1.6, and -8.5 cm^{-1}/GPa, whereas the corresponding experimental values[35] are of 3.4, 1.7, and -3.6 cm^{-1}/GPa, respectively.

The mechanism of the t-m transformation is more complicated and its understanding requires a detailed examination of the $E_c(V)$ and $E_t(V)$ curves behavior. According to results of Ref. 16, these curves smoothly merge together at the K point (see Fig. 1), whereas in Ref. 17 they intersect at the K' point. At first glance, our model gives the results (see Fig. 3) similar to those of Ref. 17: the $E_t(V)$ and $E_m(V)$ curves approach each other in point K' with different slopes which correspond to different static pressure values. However, these curves do not intersect. According to our model, there is no energy minimum in the m phase to the left of the K' point, and the $E_m(V)$ curve terminates on approaching this point from the right side. It is remarkable, that the model predicts an instability in the t phase when approaching the K' point from the left side. So, to the right of the K' point one phase (m) is stable and another one (t) is unstable, whereas to the left of the K' point only one stable phase (t) exists, somewhat similarly to the case of the c and t phases around the L point. The different slopes of $E_t(V)$ and $E_m(V)$ curves in the K' point mean that the m-t instability cannot be induced by hydrostatic compression. This can explain why the relevant phase transition was not observed.

Let us consider the microscopic origin of the instability of the t phase at volume increase. It was qualitatively shown in Ref. 22 that the vector of the t-m structural transformation would involve the combination of three phonons M_1, M_2, and E_g from which the two former correspond to the two-dimensional primary order parameter. Our model calculations confirm this issue. As it is seen from Fig. 4, the two lowest frequency M phonons soften markedly at volume expansion and both vanish eventually. The M_1 soft mode vanishes the first at the K' point. Thus, to the right of the K' point, the energy minimum in the t phase transforms into a saddle point, and the energy minimum appears in a less symmetric structure dictated by the eigenvector of the vanishing phonon. However, according to the symmetry rules, the solo condensation of the M_1 mode would transform the t phase into an orthorhombic structure with the space symmetry group $N54$ (we call it $o54$), and the solo condensation of the M_2 mode would transform the t phase into an orthorhombic structure with the space symmetry group $N60$ (α-PbO_2 structure). Only a joint condensation of these two phonons would result in the baddeleyite structure. In principle, to produce t-m transformation, it is not of importance which of those M modes vanishes the first, but both should soften on

TABLE III. Phonon frequencies (cm^{-1}) of ZrO_2 in the *c* and *t* phases.

Species		Experimental data and *ab initio* results (in brackets)		VCM, this work	
c	*t*	*c*	*t*	*c*	*t*
	B_{1u}		(673[e])		856
X_1^+		(697[e])		735	
	M_4				759
	E_g		642[d] (659[e])		677
X_5^-	M_3	(568[e])		633	644
	M_2				640
	B_{1g}		609[a] (607[e])		560
F_{2g}		490[a] (587[e])		557	
	E_g		466[d] (474[e])		506
	E_u		467[c] (479[e])		404
F_{1u}		320[b] (269[e])		334	
	A_{2u}		339[c] (339[e])		223
	M_1				335
X_4^+				218	
	B_{1g}		322[d] (339[e])		204
	M_2				249
X_5^-	M_3	(141[e])		180	231
	E_g		148[d] (147[e])		191
	E_u		164[c] (153[e])		182
X_5^+	M_2	(325[e])		170	104
	M_1				52
	A_{1g}		266[d] (259[e])		219
X_2^-		(i196[e])		i120	
	M_4				200

[a]Reference 31.
[b]Reference 28.
[c]Reference 32.
[d]Reference 33.
[e]Reference 21.

approaching the phase transition point. On testing the previous ionic models,[6,11] one can find that only the M_2 phonon softens there thus transforming the *t*-phase structure into the orthorhombic α-PbO_2 structure, but not into the monoclinic baddeleyite structure.

The origin of the softness of the M_1 and M_2 modes in our model can be understood by analyzing their eigenvectors, presented in Figs. 5(c) and 5(d) along with the atomic displacement pattern of the tetragonal-to-monoclinic transformation [Fig. 5(a)]. It is seen from Fig. 5 that the latter can be represented as a combination of the eigenvectors of the three modes M_1, M_2, and E_g. Figure 5(d) shows that the eigenvector of the M_2 mode mainly involves the relative tangential displacements of the neighboring planes of oxygen atoms. The softness of this mode can be attributed to the strong O-O repulsion giving a negative dynamic matrix contribution which arises from the high and negative value of the tangential O-O force constants. Note, that the same factor deter-

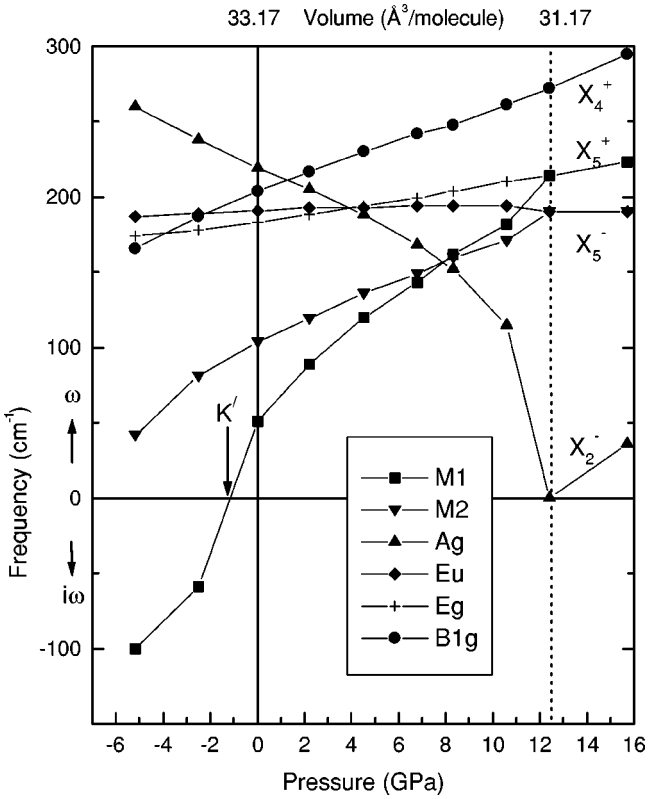

FIG. 4. Pressure and volume dependence of some phonon frequencies of tetragonal zirconia. The critical pressure wherein the *t* phase transforms into the *c* phase is shown by the dotted line. The symmetry assignment of the modes in the *c* phase is given aside.

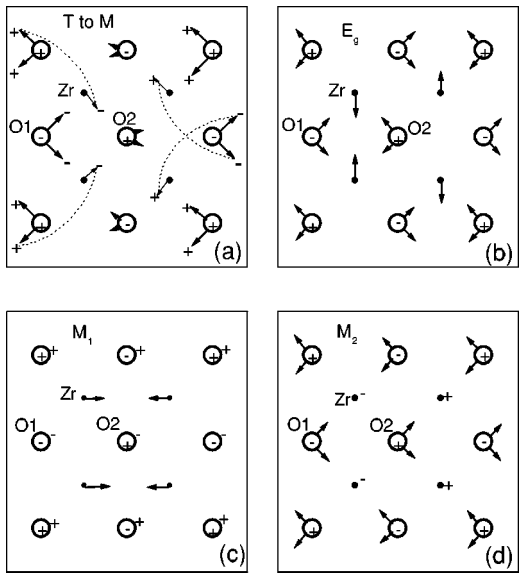

FIG. 5. *XY* projection of the atomic position rearrangement involved in the *t*-*m* transformation. (a) Eigenvectors of three modes contributing to the order parameter E_g (b), M_1 (c), and M_2 (d). The *c*-*t* distortion is shown by the plus and minus signs inside the circles, the *t*-*m* distortion is shown by arrows and by the plus and minus signs at the end of the arrows. The broken Zr-O^I bond in the *m* phase is shown by dotted curves in (a).

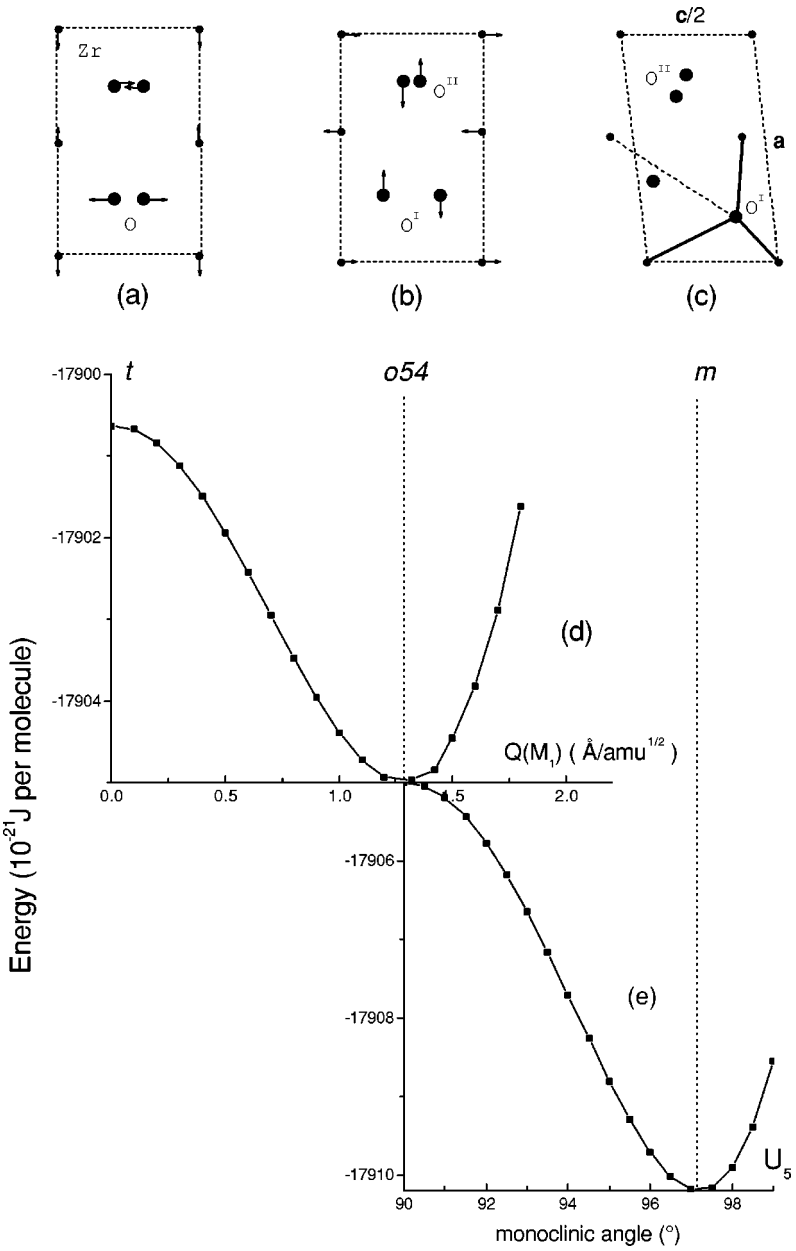

FIG. 6. XZ projection of the crystal structure in the t phase (a), $o54$ phase (b), and m phase (c); potential energy as a function of the structural distortion along the M_1-mode eigenvector (d); potential energy as a function of the orthorhombic-monoclinic distortion (e). The energy versus deformation dependences presented in this figure correspond to the potential surface cross-sections shown by the vertical arrows in Fig. 3. The broken Zr-O^{I} bond in the m phase is shown by a dotted line in plot (c).

mines the softness of X_2^- mode in the c phase.[10] This explains why the M_2 mode can be soft even within a simple ionic model.[11]

The question is why is the M_1 mode soft and why is this fact not predicted within SM but appears within VCM? On viewing Fig. 5(c), one can see that the eigenvector of this mode involves primarily the Zr atom displacements. These displacements correspond to the antiphase pulsations of the $O^{I}Zr_4$ and $O^{II}Zr_4$ tetrahedra thus resulting in the opposite sign variation of the electrostatic potentials and the charges on the O^{I} and O^{II} atoms. This explains why this mode makes the O^{I} and O^{II} atoms nonequivalent. Its condensation should produce a strong destabilizing effect due to the charge redistribution between those atoms. Since the derivatives $dZ(O^{I})/dQ(M_1)$ and $dZ(O^{II})/dQ(M_1)$ have opposite signs, the corresponding force constant contribution $dZ(O^{I})/dQ(M_1)1/|r(O^{I})-r(O^{II})|dZ(O^{II})/dQ(M_1)$ is negative.

Although the energetic criteria suggest the essentially first-order character of the t-m transition, the following structural evolution between the t and m phases can be revealed by using the soft-mode concept. As was mentioned above, the condensation of the M_1 mode would transform the t phase into the orthorhombic $o54$ structure [see Figs. 6(a) and 6(b)]. Moreover, the calculations show that the potential surface cross section along the M_1 eigenvector has a double-well form [see Fig. 6(d)] with the energy minima in the $o54$ structure. This structure is shown in Fig. 6(b), and its energy versus volume dependence is shown in Fig. 3. However, according to our calculations this $o54$ phase is essentially unstable. The shear elastic constant C_{55} and the bulk module B were found to be negative because of a strong optoacoustic coupling inherent to this structure: the lowest

frequency A_g mode (former soft M_1 mode) couples with the homogeneous strain $U_1+U_2+U_3$, and the low frequency B_{2g} mode [former soft M_2 mode, see Fig. 6(b)] couples with the U_5 strain. [The negative sign of the bulk module in the $o54$ phase is seen from the curvature of the corresponding $E_{o54}(V)$ curve in Fig. 3.] So, the $o54$ configuration corresponds to a saddle point of the potential surface. To become stable, the lattice undergoes the finite-scale spontaneous deformation including the U_5 (orthorhombic-to-monoclinic) shear deformation and the volume increment (along $U_1+U_2+U_3$) and finally evolves into the monoclinic baddeleyite structure [Figs. 6(c) and 6(e)]. Moreover, this explains why the $E_t(V)$ and $E_m(V)$ curves in Fig. 3 have no common points.

On approaching the K' point, the monoclinic structure also manifests the elastic anomalies: the elastic constants C_{55} and the bulk module values gradually vanish. This is seen in Fig. 3, in which the curvature of $E_m(V)$ tends to zero on approaching the K' point. This can be related to the nature of the tremendous volume change and shear deformation accompanying the m-t inversion.

IV. CONCLUSIONS

The main peculiarity of the atomic arrangement in zirconia, distinguishing it from other crystalline dioxides, originates from a specific value of the cation radius: it is not sufficiently large to ensure the stability of the fluoritelike cubic structure, but is too large to ensure the stability of an ''octahedral'' crystal structure with the sixfold cation coordination. Because of this peculiarity, the two principal dynamic matrix contributions, that from the Coulomb interaction and that from the overlap repulsion, are mutually canceled. As a result, the total interatomic forces in zirconia are governed by other contributions which are not prominent in most oxides as against the two major ones. The analysis of the experimental data, of the results of the *ab initio* studies, and the previous model treatments led us to conclude that the physical factor determining the stability of the baddeleyite structure is the dependence of the effective ionic charges of oxygen anions on their local environment in a lattice.

In the advanced version of the ionic model presented in this paper, the effective charges of oxygen atoms as well as their ionic radii are considered as variable values depending on the local Madelung potential. The thus developed variable charge model enables us to reproduce the main peculiarities of zirconia's potential surface, discovered in the *ab initio* studies, and to describe the structural and dynamic properties for all the zirconia polymorphs in good correspondence with the experimental data. The model calculations are capable of explaining the microscopic mechanism of both c-t and t-m instabilities. For the latter instability, the very particular two-step scenario is discovered. First, the t phase becomes unstable with respect to the zone boundary M_1 phonon mode. Consequently, it would transform into a $o54$-orthorhombic crystal structure which appears to be unstable with respect to the shear strain and volume increment simultaneously. Second, this intermediate orthorhombic structure would readily evolve into the monoclinic baddeleyite structure in undergoing a spontaneous volume increment and a shear deformation. This mechanism can be intimately related to the monoclinic-to-tetragonal structural phase transition which occurs at high temperature and also is accompanied by a spontaneous volume variation. The detailed analysis of the finite-temperature phenomena requires a consideration of the entropy contribution thus stimulating the further development of the model.

ACKNOWLEDGMENTS

This study was done while M.S. was an invited researcher in the SPCTS Laboratory (Limoges) of the Center National de la Recherche Scientifique of France, and he would like to thank the staff for hospitality and helpful discussions. The authors express a particular gratitude to Professor J.-F. Baumard for his help and encouragement. The participation of M.S. in the work was partly supported by the Basic Research Russian Foundation (Grant No. 00-03-33040).

*Author to whom correspondences should be addressed. Email address: andrem@unilim.fr

[1] D.J. Green, R.H.J. Hannink, and M.V. Swain, *Tranformation Toughening of Ceramics* (CRC Press, Boca Raton, FL, 1988).
[2] E.H. Kisi and C.J. Howard, in *Zirconia Engineering Ceramics: Old Challenges-new Ideas*, edited by E.H. Kisi (Trans Tech, Netikon-Zurich, 1998).
[3] P. Bouvier, E. Djurado, G. Lucazeau, and T. Le Bihan, Phys. Rev. B **62**, 8731 (2000).
[4] L.L. Boyer and B.M. Klein, J. Am. Ceram. Soc. **68**, 278 (1985).
[5] R.E. Cohen, M.J. Mehl, and L.L. Boyer, Physica B **150**, 1 (1988).
[6] A. Dwivedi and A.N. Cormack, Philos. Mag. A **61**, 1 (1990).
[7] E.V. Stefanovich, A.L. Shlunger, and C.R.A. Catlow, Phys. Rev. B **49**, 11 560 (1994).
[8] Y. Zhou and H.J.F. Jansen, Bull. Am. Phys. Soc. **38**, 674 (1993).
[9] G.W. Fernando, E.H. Sevilla, J.A. Rifkin, and P.C. Clapp, Bull. Am. Phys. Soc. **38**, 674 (1993).
[10] M. Wilson, U. Schönberger, and M.W. Finnis, Phys. Rev. B **54**, 9161 (1996).
[11] A.P. Mirgorodsky, M.B. Smirnov, and P.E. Quintard, J. Phys. Chem. Solids **60**, 985 (1999).
[12] H.J.F. Jansen and J.A. Gardner, Physica B **150**, 10 (1988).
[13] H.J.F. Jansen, Phys. Rev. B **43**, 7267 (1991).
[14] R. Orlando, C. Pisani, C. Roetti, and E. Stefanovich, Phys. Rev. B **45**, 592 (1992).
[15] J.K. Dewhurst and J.E. Lowther, Phys. Rev. B **57**, 741 (1998).
[16] A. Christensen and E.A. Carter, Phys. Rev. B **58**, 8050 (1998).
[17] G. Jomard, T. Petit, A. Pasturel, L. Magaud, G. Krese, and J. Hafner, Phys. Rev. B **59**, 4044 (1999).
[18] J.E. Lowther, J.K. Dewhurst, J.M. Leger, and J. Haines, Phys. Rev. B **60**, 14 485 (1999).
[19] K. Parlinski, Z.Q. Li, and Y. Kawazoe, Phys. Rev. Lett. **78**, 4063 (1997).
[20] F. Detraux, Ph. Ghosez, and X. Gonze, Phys. Rev. Lett. **81**, 3297 (1998).
[21] G.M. Rignanese, F. Detraux, X. Gonze, and A. Pasquarello, Phys. Rev. B **64**, 134301 (2001).

[22] K. Negita and H. Takao, J. Phys. Chem. Solids **50**, 325 (1989).
[23] G.I. Kramer, N.P. Farragher, and B.W.H. van Best, Phys. Rev. B **43**, 5068 (1991).
[24] In Ref. 10, it became possible to obtain an energy minimum in the monoclinic phase only after introducing the quardrupole polarizability and the dipole-dipole-quadrupole hyperpolarizability. However, the stability of this structure was not analyzed.
[25] M. Born and K. Huang, *Dynamical Theory of Crystal Lattices* (Oxford University Press, Oxford, 1954).
[26] K. Negita, Acta Metall. **37**, 313 (1989).
[27] A.D.B. Woods, W. Cochran, and B.N. Brockhause, Phys. Rev. **119**, 980 (1960).
[28] D.W. Liu, C.H. Perry, A.A. Feinberg, and R. Currat, Phys. Rev. B **36**, 9212 (1987).
[29] V. Kuznetsov (private communication).
[30] A.K. Rappe and W.A. Goddard III, J. Phys. Chem. **95**, 3358 (1991).
[31] C.M. Philippi and K.S. Mazdiyasni, J. Am. Ceram. Soc. **70**, 284 (1971).
[32] C. Pecharroman, M. Ocana, and C.J. Serna, J. Appl. Phys. **80**, 3479 (1996).
[33] T. Merle, R. Guinebretiere, A. Mirgorodsky, and P. Quintard, Phys. Rev. B **65**, 144302 (2002).
[34] O. Ohtaka, T. Yamaka, and T. Yagi, Phys. Rev. B **49**, 9295 (1994).
[35] P. Bouvier and G. Lucazeau, J. Phys. Chem. Solids **61**, 569 (2000).